American Mineralogist, Volume 90, pages 502–505, 2005

LETTER

Very low solubility of rutile in H_2O at high pressure and temperature, and its implications for Ti mobility in subduction zones

PETER TROPPER[1,2] AND CRAIG E. MANNING[2,*]

[1]Institute of Mineralogy and Petrography, University of Innsbruck, Innrain 52, A-6020 Innsbruck, Austria
[2]Department of Earth and Space Sciences, University of California, Los Angeles, California 90095-1567, U.S.A.

ABSTRACT

The solubility of rutile in H_2O has been measured at 1000–1100 °C, 1–2 GPa. The data indicate that solubility is very low over the investigated range, with a maximum of 4.7 millimol/kg H_2O at 1100 °C, 2 GPa. The data were fit with the equation $\log m_{Ti} = 4.892–10470/T + 0.1923P$, where m_{Ti} is Ti molality, T is in Kelvins, and P in GPa. When compared to previous results, the new data indicate substantially lower solubility, opposite pressure dependence, and thermodynamic properties of the reaction rutile = $TiO_{2,aq}$ that are now consistent with other oxide hydrolysis reactions. Calculations of Ti transport during mantle metasomatism by H_2O in subduction zone environments predict much lower Ti mobility at all conditions. These results offer strong support for models of Ti retention in eclogites during slab devolatilization, and require that examples of significant Ti mass transfer be explained by complexing agents in solution, most likely aluminosilicate complexes.

INTRODUCTION

Rutile (TiO_2), a common accessory mineral in eclogites and other high-pressure rocks (e.g., Philippott and Selverstone 1991; Van Baalen 1993; Rubatto and Hermann 2003), plays a central role in controlling the distribution high-field-strength elements (HFSE) in the Earth (Kamber and Collerson 2000; Rudnick et al. 2000). A key step in the terrestrial cycling of Ti (and other HFSE) occurs in subduction zones. There, fluid-rock interaction leads to retention of these elements in eclogitic rutile, producing a Ti-enriched reservoir that is subducted into the deep Earth, and complementary Ti-depleted arc magmas that are returned to the surface (Brenan et al. 1994; Foley et al. 1999; Rudnick et al. 2000). This model is based in part on the widely held view that the solubility of rutile is quite low in H_2O-rich subduction-zone fluid.

However, the assumption of low rutile solubility in H_2O is problematic. Experimental data suggest that the solubility of rutile in H_2O may actually be relatively high (Ayers and Watson 1993). For example, at 1000 °C, 1 GPa, the data of Ayers and Watson (1993) indicate that Ti concentration at rutile saturation is 0.2 molal, or >50 times more soluble than Al at corundum saturation (Tropper and Manning 2004), and similar in magnitude to the solubility of quartz in H_2O at mid-crustal metamorphic conditions (e.g., ~600 °C, 0.5 GPa; Manning 1994). Moreover, Ayers and Watson (1993) found that rutile solubility decreases strongly with increasing pressure (P) at constant temperature (T). This result differs from other simple minerals such as quartz, corundum, calcite, and anhydrite (Manning 1994; Caciagli and Manning 2003; Newton and Manning 2004; Tropper and Manning 2004). Such behavior would greatly enhance Ti transport by H_2O moving from slab to wedge, and lead to rutile precipitation near the arc-magma source region (Ayers and Watson 1993). Rutile formation in the mantle wedge reduces the retention of Ti in eclogites and is inconsistent with the high rutile solubility and low Ti contents of arc basalts (Ryerson and Watson 1987). Thus, whereas complexing with other ligands and dissolved silicate may also influence Ti mobility in subduction zones, the existing data on the solubility of rutile in H_2O pose a fundamental dilemma.

To address this problem, we measured the solubility of rutile in H_2O at 1000–1100 °C, 1–2 GPa. The new data indicate that rutile solubility is significantly lower than given by previous solubility measurements, and that the P dependence of solubility is opposite in sign. These results indicate that dilute aqueous solutions have an extremely low capacity to dissolve and transport Ti at high P and T, which supports models of HFSE retention in the slab during devolatilization.

EXPERIMENTAL METHODS

Two types of rutile were used as starting materials. Initial experiments were conducted with sintered rutile made by firing TiO_2 powder (Fisher Co.) at 1000 °C over three days, with repeated grinding. X-ray diffraction verified the absence of additional phases. In subsequent experiments, we used pure, transluscent, clear-to-yellowish, flux-grown rutile crystals, with lattice constants of $a = 4.5933$ Å and $c = 2.9592$ Å.

In experiments using sintered rutile, the powder was pressed into a small pellet and placed in an inner Pt capsule, which was welded at one end, crimped at the other, and multiply punctured to facilitate H_2O penetration. The capsule and ~35 µL H_2O were then sealed in a welded Pt capsule with 3.5 mm OD, 0.20 mm wall thickness, and held at 115 °C for ≥3 h to check for leakage. In experiments on single crystals, a polished chip of flux-grown rutile was placed in a folded Pt-envelope, which was lightly crimped to allow H_2O entry. Loading procedures were otherwise identical. We initially omitted the inner capsule from experiments on single crystals, but occasional breakage and significant growth of new grains during runs indicated that the second capsule was needed to segregate the starting rutile from the main fluid reservoir and to minimize TiO_2 transport during experiment (see below).

All experiments were conducted in an end-loaded, piston-cylinder apparatus using 25.4 mm diameter furnace assemblies. Each capsule was placed horizontally in the furnace, packed in NaCl or BN, and covered with a piece of Pt foil to prevent puncture by the thermocouple. Experiments below the NaCl melting curve employed graphite-NaCl furnace assemblies (Bohlen 1984). Furnaces in

* E-mail: manning@ess.ucla.edu,

0003-004X/05/0203–502$05.00/DOI: 10.2138/am.2005.1806

experiments at 1.0 GPa, ≥1000 °C, included BN interior pieces and pre-cracked Pyrex sleeves on the graphite heater. Pre-cracking, which was necessary to reduce furnace-assembly strength so that *P* on the capsule was maximized during run up, was achieved by heating sleeves to 800 °C for 5 min and quenching in cold water. A friction correction of –20% of the nominal gauge pressure was applied to experiments with these assemblies. Temperature was controlled with $Pt/Pt_{90}Rh_{10}$ thermocouples (±3 °C estimated precision), and pressure was monitored using a Heise gauge (±0.01 GPa estimated precision).

Experiments were quenched to <100 °C in ≤30 s. After quenching, the capsule was pierced with a needle, dried for 15 min at 115 °C, and then 15 min at 400 °C. The capsule was then opened and inspected, and the rutile extracted and weighed.

Checks of H_2O weight confirmed no significant loss during runs. Weighings were made with a Mettler M3 microbalance. Propagations of weighing error gave $1\sigma = 0.6$ millimolal and minimum detection limit at the 95% confidence level of 2 μg.

RESULTS

Results are given in Table 1. Run products included three morphologies of rutile crystals. Original, starting grains showed rounded edges, low-relief scalloping, and in some cases, surface recrystallization in the form of small stubby, prisms (Fig. 1A). Chips of flux-grown rutile change from colorless to indigo blue during experiments, probably because of Ti^{4+} reduction to Ti^{3+} with accompanying OH substitution at trace levels (Withers et al. 2003).

A second run-product morphology is fine, acicular, colorless needles that are randomly distributed primarily in the outer capsule (Fig. 1B). The needles may be >100 μm long, and range from sparse crystallites to dense, fibrous mats and clumps. Abundance increases with *T* (i.e., expected solubility). Because of their morphology, high nucleation density, distribution, and abundance, we interpret acicular needles as quench material.

The third type of product rutile was blocky, equant to prismatic, brownish to blue crystals. These grains grew in some, but not all experiments. They formed at the ends of the outer capsules, which were the coldest spots during experiments. They typically occur as polycrystalline clumps ranging from 10 to 150 μm in longest dimension (Fig. 1C), although a single prismatic grain with fluid inclusions (Fig. 1D) grew in Rt-33 and Rt-34 (1100 °C, 1 GPa; Table 1). Because they grew in cold spots and show low nucleation density, these crystals are interpreted to have grown during experiment by aqueous TiO_2 transport in the small *T* gradient in the capsule. Four observations support this interpretation. First, apparent solubility at a given *P* and *T* was always higher when these crystals were present (Table 1). In addition, at a given *P* and *T*, this type of crystal tended to increase in abundance with time (Table 1). Third, we initially found that abundant growth of "transport" crystals occurred when the inner capsule was omitted. Including an inner Pt envelope greatly reduced, but did not always eliminate, transport-crystal growth, probably because of higher heat conduction in the capsule interior. Finally, in the one instance in which a transport crystal was large enough to be collected and weighed (Rt-33, Table 1), the resulting solubility was consistent with values extrapolated from lower *T*. Similar crystals were identified by Caciagli and Manning (2003) in their study on calcite solubility in H_2O.

Formation of quench crystals does not affect solubility determination because the starting material is held in the inner capsule and easily separated for weighing; however, the transport crystals are problematic because they were generally too small to be collected and weighed with confidence. Short run times and addition of an inner Pt envelope most effectively minimized growth of transport crystals (Table 1), but it proved impossible to suppress the process consistently, evidently because of subtle geometric differences from run to run. Thus, experiments in which transport growth occurred yielded erroneously high solubilities and were

TABLE 1. Results of experiments on rutile solubility in H_2O

Run	Methods*	*P* (GPa)†	*T* (°C)	Time (h)	H_2O (mg)	Rt in (mg)	Rt out (mg)	logm_{Ti}‡	Quench xls§	Transport xls§
Experiments unaffected by transport crystals										
RT-1	C1 X2 A1	1.0	800	14	32.053	1.079	1.079	b.d.	-	-
RT-4	C1 X1 A1	1.0	800	25	33.457	1.843	1.843	b.d.	-	-
RT-3	C1 X2 A1	1.0	900	24	34.398	1.719	1.719	b.d.	-	-
RT-32	C2 X1 A2	1.0	1000	12	36.848	0.548	0.546	–3.17(35)	+	-
RT-33	C2 X1 A2	1.0	1100	12	36.884	1.600	1.591	–2.52(01)	++	+++‖
RT-10	C2 X1 A1	2.0	1000	1	34.987	2.842	2.849	b.d.	-	-
RT-29	C2 X1 A1	2.0	1000	8	36.630	1.889	1.885	–2.86(18)	+	-
RT-30	C2 X1 A1	2.0	1000	12	36.083	1.489	1.486	–2.98(24)	+	-
RT-26	C2 X1 A1	2.0	1050	12	36.351	1.699	1.693	–2.86(12)	++	-
RT-24	C2 X1 A1	2.0	1100	2	35.035	1.911	1.906	–2.75(14)	+++	-
RT-27	C2 X1 A1	2.0	1100	8	36.975	3.047	3.033	–2.32(05)	+++	-
RT-31	C2 X1 A1	2.0	1100	12	35.890	1.567	1.555	–2.38(06)	+++	-
Experiments yielding transport crystals										
RT-9	C0 X1 A1	1.0	900	53	34.956	2.891	2.883	*–2.54(09)*	-	++
RT-7	C0 X1 A1	1.0	1000	2.5	34.415	2.085	2.074	*–2.40(06)*	+	+++
RT-8	C0 X1 A1	1.0	1000	21	34.188	2.868	2.686	*–1.18(01)*	+	+++
RT-34	C2 X1 A1	1.0	1100	12	36.923	0.696	0.684	*–2.39(06)*	++	+
RT-28	C2 X1 A1	2.0	1000	2	36.657	1.331	1.327	*–2.86(18)*	-	++
RT-11	C2 X1 A1	2.0	1000	16	35.055	2.402	2.397	*–2.75(14)*	++	+
RT-18	C0 X1 A1	2.0	1000	24	35.095	3.738	3.722	*–2.24(04)*	++	+
RT-21	C2 X1 A1	2.0	1000	24	36.919	2.314	2.306	*–2.57(09)*	+	+
RT-20	C2 X1 A1	2.0	1100	24	36.362	3.065	3.016	*–1.77(01)*	+++	++

* Inner capsule types: C0, none; C1, welded and punctured capsule; C2, Pt envelope. Starting rutile: X1, flux-grown single crystal chips; X2, sintered TiO_2. Furnace assembly types: A1 = NaCl-graphite assembly; A2 = High-temperature NaCl-graphite-Pyrex-BN assembly.

† Experiments using A2 assemblies run at nominal gauge-pressure of 1.2 GPa and a -0.2 GPa friction correction was applied.

‡ Solubility is expressed as logarithm of Ti molality (m_{Ti}): $m_{Ti} = 1000\Delta_w/(M_{TiO_2}w_{H_2O})$], where Δ_w is rutile mass change, M_{TiO_2} is the molecular weight of TiO_2 (79.8988 g) and w_{H_2O} is the weight of the fluid after experiment. b.d. = below detection limit (2 μg). Italics signify spurious, apparent solubility caused by presence of transport crystals. Parenthetical numbers are propagated 1σ weighing errors.

§ Qualitative abundance of quench and transport crystals: none (–), sparse (+), moderate (++), and abundant (+++).

‖ Transport crystal was retrieved and weighed with starting crystal.

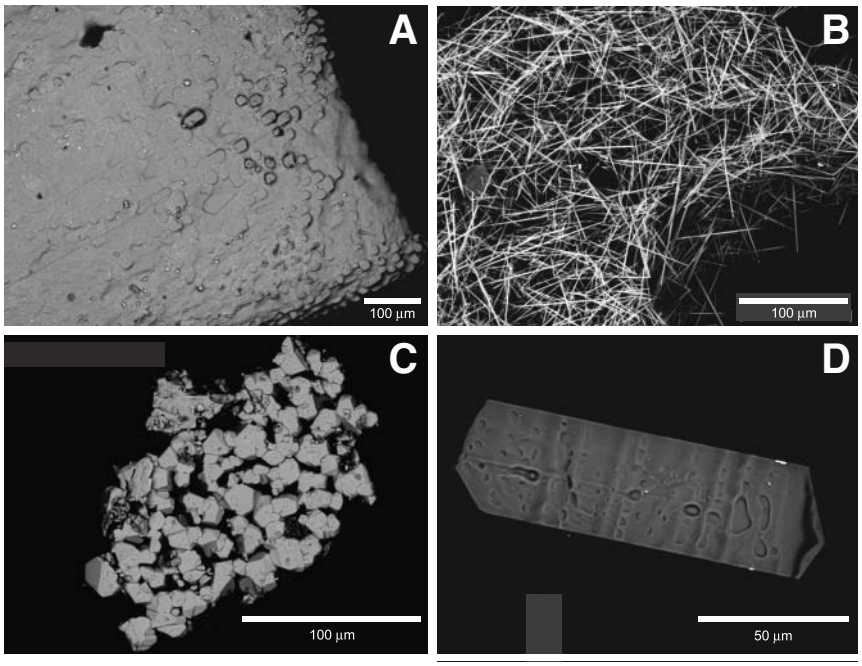

FIGURE 1. Back-scattered electron (BSE) images of the reaction products after the solubility experiments. (**a**) Recrystallization texture showing newly grown rutile crystals on the surface of the starting chip (Rt-33). (**b**) Aggregate of quench crystals of rutile in experiment Rt-24. Note, within the needles, a blocky vapor-transport rutile crystal occurs. (**c**) An aggregate of blocky vapor-transport rutile crystals from experiment Rt-8. (**d**) Prism-shaped vapor-transport crystal with fluid inclusions from experiment Rt-33.

discounted (Table 1).

Run duration necessary to attain equilibrium was determined in two sets of experiments at 2 GPa, 1000 and 1100 °C (Fig. 2). In both sets of experiments, constant solubility within uncertainty was reached by 8 h. Runs longer than 12 h led to growth of transport crystals at ≥1000 °C (Table 1). Equilibrium solubility was always approached from undersaturation.

The equilibrium solubility of rutile in H_2O is very low at the *P* and *T* of this study. Aqueous Ti concentrations ranged from below detection (<2 µg weight change) to 4.7±0.6 millimolal (Table 1). Rutile solubility increases with *T* at 1 and 2 GPa (Fig. 3). The results suggest a slight increase in solubility with *P*.

DISCUSSION

A fit to the equilibrium rutile solubility data gives $\log m_{Ti} = 4.892 - 10470/T + 0.1923P$, where *T* is in Kelvins and *P* in GPa (Fig. 3). The slight positive *P* dependence implied by the fit equation is consistent with the data at 1 and 2 GPa, but its magnitude is highly uncertain.

The results of this study differ from those of Ayers and Watson (1993) in two important ways (Fig. 3): they reported rutile solubility in H_2O up to 270 times higher at the same *P* and *T*, and their results indicate a decrease in solubility with increasing *P* and constant *T*. Ayers and Watson (1993) used a large capsule design, which had a significant *T* gradient. Their Figure 2A shows blocky crystals similar to the transport crystals grown during our experiments, which they interpreted as quench. Ayers and Watson (1993) acknowledged growth of transport crystals at ≥1100 °C, and concluded that their data represented maximum values. The present data set suggests that transport and redeposition actually affected all of their results.

The data of the present study resolve several problematic implications of the results of Ayers and Watson (1993). First, the

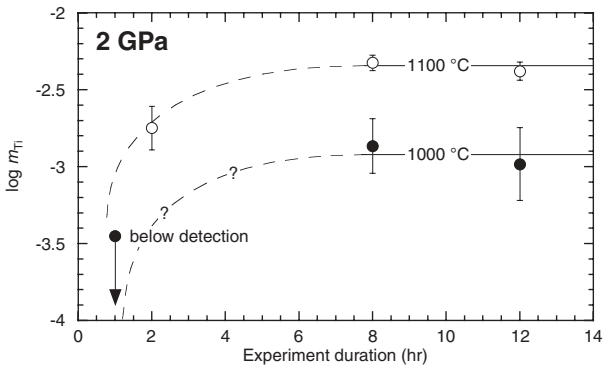

FIGURE 2. Variation in rutile solubility with time at 1GPa, 1000 °C (**a**) and 1100 °C (**b**). Error bars are 1σ based on propagation of weighing uncertainties.

new results translate to thermodynamic properties of the equilibrium $TiO_{2,rutile} = TiO_{2,aq}$ that are more similar to those of other oxide-dissolution reactions at high *P*. Assuming only neutral $TiO_{2,aq}$ with unit activity coefficient, the slight positive *P* dependence found at the *P* and *T* studied indicates a negative ΔV_r° of –4.7 to –5.1 cm^3/mol, as opposed to +11.3 cm^3/mol derived from the fit equation of Ayers and Watson (1993). Negative ΔV_r° is more consistent with the expectation that Ti hydration by H_2O yields lower product volume, which leads to an isothermal increase in solubility with *P*, similar to other oxides. For example, corundum ($AlO_{1.5}$) solubility at 700 °C suggests ΔV_r° for dissolution to $AlO_{1.5,aq}$ at 2 GPa is –4.43 cm^3/mol (Becker et al. 1983). Similarly, the results of Manning (1994) on quartz-$SiO_{2,aq}$ equilibrium yield $\Delta V_r^\circ = -3.70$ cm^3/mol at 1000 °C, 2 GPa. In addition, the lower measured solubility implies that the Gibbs free energy of the reaction is 39–56 kJ/mol more positive than is suggested by the

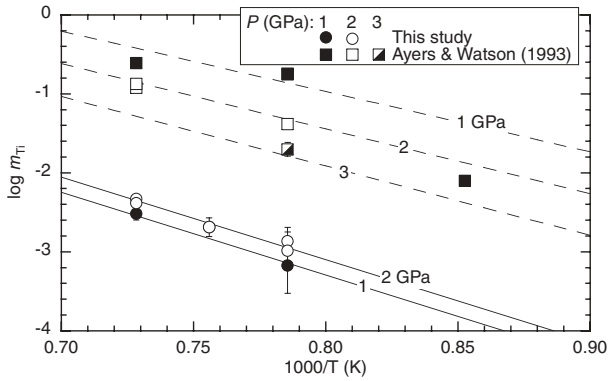

FIGURE 3. Variation of Ti molality with inverse *T* (Kelvins). Data from this study are shown in circles; data from Ayers and Watson (1993), in squares. Solid lines were calculated from the empirical fit to data of this study (see text); dashed lines are from the Equation 3 of Ayers and Watson (1993).

data of Ayers and Watson (1993). Because the derived reaction entropies are similar [~100 J/(mol·K)], rutile-$TiO_{2,aq}$ equilibrium is more endothermic than previously indicated.

More importantly, the new results demonstrate that wedge metasomatism by pure H_2O has an extremely low capacity to modify mantle Ti concentration, and by extension HFSE. Decreasing solubility with increasing *P* (Ayers and Watson 1993) would indicate that isothermally rising H_2O would strip progressively larger quantities of TiO_2 from rutile-saturated rock. For example, for upflow at 1100 °C, flux of 1 kg H_2O/m^2 would remove 580 ppm Ti per m^3 of rock assuming 1 GPa, rutile saturation, and ρ_{rock} = 310 kg/m^3 based on results and equations of Ayers and Watson (1993). By contrast, the data of the present study indicate *addition* of 2 ppm Ti at the same conditions. These differences arise from the opposite *P* dependence of solubility in the two studies. Extrapolating the results to rutile-saturated flow of H_2O from the slab (600 °C, 3 GPa) upward into the mantle wedge (1100 °C, 2 GPa; Manning 2004a), the new data predict progressive loss of Ti of 0.01 to 41 ppm per m^3 of rock along this path. More extensive Ti loss of 0.25 to 1314 ppm is predicted by the Ayers and Watson (1993) data on the same path. The sign of Ti mass transfer is the same in this comparison because both studies yield strong, positive *T* dependence of solubility that outweighs the minor (and opposite) *P* dependencies. Differences in magnitude result from the large solubility contrasts between the data sets.

Data on the solubility of rutile in H_2O are important for establishing the properties of $TiO_{2,aq}$. The present results show that this species will have low concentration in H_2O at virtually all subduction-zone conditions in both the slab and the mantle wedge. However, instances of Ti mass transfer have been inferred in high-pressure rocks (e.g., Philippot and Selverstone 1991; Van Baalen 1993; Rubatto and Hermann 2003). Although strong departures from near-neutral pH and complexing ligands such as F can enhance Ti solubility (Van Baalen, 1993), these conditions are unlikely to be widespread in high-*P* environments. Experimental studies on Ti-bearing ultramafic-H_2O systems (Schneider and Eggler 1987; Ayers et al. 1997) have revealed higher Ti solubility than were determined here. If correct, higher Ti solubility in silicate-bearing solutions than in pure H_2O would strongly suggest that Ti solubility and mobility can be enhanced by complexing with polymerized silicate molecules in solution (Manning 2004b).

ACKNOWLEDGMENTS

We thank R. Stalder and R. Dymek for reviewing the manuscript, E. Essene for the flux-grown rutile, A. Antignano IV, and R. Newton for experimental help, and R. Tessadri for performing the X-ray refinement of the rutile starting material. Comments by R. Newton and J. Brenan improved early drafts of the manuscript. Supported by NSF grants EAR 9909583 and 0337170.

REFERENCES CITED

Ayers, J.C. and Watson, E.B. (1993) Rutile solubility and mobility in supercritical aqueous fluids. Contributions to Mineralogy and Petrology, 114, 321–330.

Ayers, J.C., Dittmer, S.K., and Layne, G.D. (1997) Partitioning of elements between peridotite and H_2O at 2.0–3.0 GPa and 900–1100 °C, and application to models of subduction zone processes. Earth and Planetary Science Letters, 150, 381–398.

Becker, K.H., Cemic, C., and Langer, K.E.O.E. (1983) Solubility of corundum in supercritical water. Geochimica et Cosmochimica Acta, 47, 1573–1578.

Bohlen, S.R. (1984) Equilibria for precise pressure calibration and a frictionless furnace assembly for the piston-cylinder apparatus. Neues Jahrbuch für Mineralogie, Monatshefte, 9, 404–412.

Brenan, J.M., Shaw, H.F., Phinney, D.L., and Ryerson, F.J. (1994) Rutile-aqueous fluid partitioning of Nb, Ta, Hf, Zr, U and Th: implications for high field strength element depletions in island-arc basalts. Earth and Planetary Science Letters, 128, 327–339.

Caciagli, N.C. and Manning, C.E. (2003) The solubility of calcite in water at 5–16 kbar and 500–800 °C. Contributions to Mineralogy and Petrology, 146, 275–285

Foley, S.F., Barth, M.G., and Jenner, G.A. (1999) Rutile/melt partition coefficients for trace elements and an assesment of the influence of rutile on the trace element characteristics of subduction zone magmas. Geochimia et Cosmochimia Acta, 64, 933–938.

Kamber, B.S. and Collerson, K.D. (2000) Role of 'hidden' deeply subducted slabs in mantle depletion. Chemical Geology, 166, 241–254.

Manning, C.E. (1994) The solubility of quartz in H_2O in the lower crust and upper mantle. Geochimica et Cosmochimica Acta, 58, 4831–4839.

——— (2004a) The chemistry of subduction-zone fluids. Earth and Planetary Science Letters, 223, 1–16

——— (2004b) Polymeric silicate complexing in aqueous fluids at high pressure and temperature, and its implications for water-rock interaction. In R.B. Wanty and R.R. Seal II, Eds., Water-Rock Interaction, 45–49. Balkema, New York.

Newton, R.C. and Manning, CE. (2005) Solubility of anhydrite, $CaSO_4$, in NaCl-H_2O solutions at high pressures and temperatures: applications to fluid-rock interaction. Journal of Petrology, in press.

Philippot, P. and Selverstone, J. (1991) Trace element-rich brines in eclogitic veins: implications for fluid compositions and transport during subduction. Contributions to Mineralogy and Petrology, 106, 417–30.

Rubatto, D. and Hermann, J. (2003) Zircon formation during fluid circulation in eclogites (Monviso, Western Alps): implications for Zr and Hf budget in subduction zones. Geochimica et Cosmochimica Acta, 67, 2173–187.

Rudnick, R.L., Barth, M., Horn, I., and McDonough, W.F. (2000) Rutile-bearing refractory eclogites: missing link between continents and depleted mantle. Science, 287, 278–81.

Ryerson, F.J. and Watson, E.B. (1987) Rutile saturation in magmas: implications for Ti-Nb-Ta depletion in island arc basalts. Earth and Planetary Science Letters, 86, 225–39.

Schneider, M.E. and Eggler, D.H. (1986) Fluids in equilibrium with peridotite minerals: implications for mantle metasomatism. Geochimica et Cosmochimica Acta, 50, 711–24.

Tropper, P. and Manning, C.E. (2004) The solubility of rutile and corundum in H_2O at high P and T: Constraints on Ti and Al mobility during high-P metamorphism. Lithos, 73 (Supplement), S113.

Van Baalen, M.R. (1993) Titanium mobility in metamorphic systems: a review. Chemical Geology, 110, 233–49.

Withers, A.C., Essene, E.J., and Zhang, Y. (2003) Rutile/TiO_2II phase equilibria. Contributions to Mineralogy and Petrology, 145, 199–04.

MANUSCRIPT RECEIVED SEPTEMBER 3, 2004
MANUSCRIPT ACCEPTED OCTOBER 21. 2004
MANUSCRIPT HANDLED BY ROBERT F. DYMEK